Scanning the Magnetic Field of Electro-dynamic Transducers

Wolfgang Klippel, wklippel@klippel.de

The magnetic flux density in the magnetic gap and the geometry of the moving coil determine the force factor *Bl* which is an important parameter of the electro-dynamical transducer. The paper presents a new measurement technique for scanning the flux density *B(z, φ)* on a cylindrical surface within and outside the magnetic gap using a Hall sensor and robotics which moves the position of the sensor along vertical position *z* and angle *φ*. The results derived from the scanning process reveal the real *B*-field in the gap considering the fringe field and irregularities in the magnetization, which can initiate a rocking mode and rubbing of the voice coil at higher amplitudes. Using the geometry of the coil the static force factor *Bl(x, i=0)* can be calculated as a function of voice coil displacement *x* and compared to the dynamic force factor *Bl(x,i>0)* measured by dynamic system identification. Discrepancies between dynamic and static force factor characteristics are discussed and conclusions for loudspeaker design and manufacturing are derived.

INTRODUCTION

Most loudspeakers use a voice coil in the magnetic field to generate a Lorenz force driving the mechanical system. One of the most important lumped parameter of the electro-dynamical transducer is the force factor

$$Bl = \mathbf{e}_z \cdot \int_l \mathbf{B}(\mathbf{r}_l) \times d\mathbf{r}_l \qquad (1)$$

which is the integral of the magnetic flux density **B** over all points $\mathbf{r}_l$ on the voice coil wire with the total length *l*. The magnitude and direction of the vector **B** at all relevant field points $\mathbf{r}_l$ determines the force factor value *Bl(x=0)* at the rest position z_r and the force factor nonlinearity *Bl(x)* for any voice coil displacement *x*.

Figure 1 illustrates the measurement of the force factor *Bl(x)* either by integrating the magnetic flux density [1] or by identifying the lumped parameter in the assembled transducer [2-6].

The DC flux density $\mathbf{B}(\mathbf{r}_l, i_{coil}=0)$ generated by the permanent magnet without any voice coil current i_{coil} can be determined by finite element modeling (magnetic FEM [7]) or direct measurement [8]. The manual measurement is time consuming and an exact positioning of the sensor at defined points difficult. The development of an automatic scanning technique for the magnetic flux density in the gap of loudspeakers is the first objective of this paper. The two-dimensional data provided by the scanning process require new derived characteristics to simplify the interpretation and to provide essential information for loudspeaker diagnostics. Finally the influence of the voice coil current i_{coil} on the measured force factor characteristic $Bl(x, i_{coil})$ is investigated by comparing the results derived from the static measurement of the B field with the results of nonlinear system identification applied to the assembled transducer.

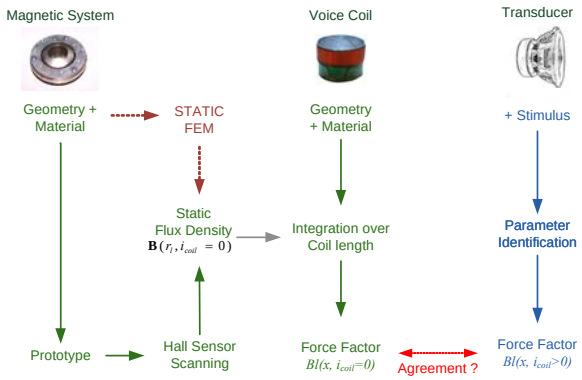

Figure 1: Measurement of characteristics of the magnetic field

SYMBOLS

$B(z_i, \varphi_k, r_0)$	Magnetic flux density in radial direction at a scanning point defined in cylindrical coordinates
$B(z, \varphi)$	Magnetic flux density in radial direction interpolated on the cylindrical scanning surface

$\overline{B}^{z}(\varphi)$	Mean value of magnetic flux density averaged over the vertical scanning coordinate z versus circumferential angle φ
$\overline{B}^{\varphi}(z)$	Mean value of magnetic flux density averaged over circumferential angle φ versus vertical coordinate z
$\overline{\overline{B}^{\varphi}}^{z}$	Mean value of magnetic flux density averaged over the scanned cylindrical surface
$Bl(x)$	Force factor as function of voice coil displacement x
$Bl'(x,\varphi)$	Force factor density on the circumference in the magnetic gap
$\mathbf{B}(\mathbf{r}_l)$	Flux density vector (induction) at point $\mathbf{r}_l$ on the coil wire
b	Width of the Hall sensor
D	Diameter of the voice coil wire with insulation
$\mathbf{e}_z$	Unit vector pointing in vertical z direction corresponding with cone displacement
l	Total length of the voice coil wire
i_{coil}	Voice coil current
I_0	Constant DC current supplied to the Hall sensor
m	Number of layers of the voice coil
φ_k	Angle describing the position of the point k on the scanned cylindrical surface
N_w	Number of windings in each voice coil layer
N_z	Number of scanning points in vertical direction
N_φ	Number of scanning points on the circumference
r_0	Radius of a circumference in the middle of the gap
R_H	Hall constant
U_H	Output voltage of the Hall sensor
$V_B(z,\varphi)$	Relative variation of the magnetic flux density
W	Width of the gap
x	Displacement of the voice coil
z_H	Height of the cylindrical surface scanned
z_i	Vertical coordinate of a scanned point i on cylindrical surface
z_r	Rest position of the voice coil

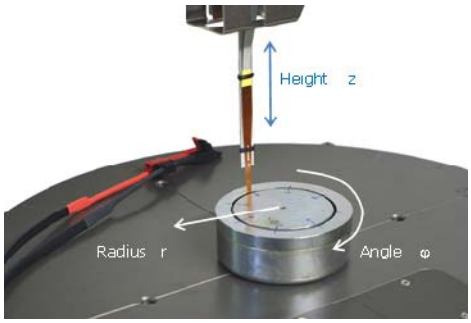

Figure 2: Measurement of the magnetic flux density in the gap by using a Hall sensor and a mechanical scanning system.

MEASUREMENT OF THE PERMANENT FIELD

The direct measurement of the magnetic flux density B penetrating the voice coil wire at any point in the gap requires free access to the magnetized magnetic system (pole piece, back plate, magnet). This can be achieved by removing the voice coil and diaphragm of an assembled drive unit. The width of the magnetic gap is relatively small (about 1 mm) compared to the gap depth and a probe is required which should be thin and long to be placed at any point in the gap.

This task can be accomplished by a search-coil which measures the magnetic flux by integrating the back-induced electro-magnetic force (EMF) generated in the coil while moving the coil through the magnetic field. The size of the coil and a potential drift of the integrator make the flux-meter less useful for scanning application [1].

Hall-Effect Sensor

The Hall-effect sensor measures the magnetic flux density more directly and generates a Hall voltage

$$U_H = R_H \cdot \frac{I_o \cdot B}{b} \tag{2}$$

proportional to the radial component of the flux density B and an electric supply current I_0. Sensitive probes should use Hall elements having a small width b and a large Hall coefficient R_H mounted on a narrow flexible circuit board to simplify the electrical connection. The probe depicted in Figure 2 has a thickness of 0.5 mm and width of 3.2 mm only and can be injected more than 50 mm into the gap while providing a sensitivity of 0.1 V/T which is sufficient for most applications.

Scanning Technique

An accurate measurement of the B-field requires a precise positioning of the Hall sensor in vertical direction z (height) because the B-field varies strongly at both ends of the gap. The variation versus the angle φ is moderate and the B-field is almost independent of the radius r within the gap. The sensor should have sufficient mechanical stiffness to ensure a proper r dimension when

the sensor leaves the gap and is not guided by the pole plates anymore.

A mechanical scanner system originally developed for the measurement of cone vibration [9] has been modified for magnetic scanning. Experiments have been performed to find a scanning grid giving sufficient resolution and keeping the measurement time as short as possible. A sufficient angular resolution requires 4 to 10 points N_φ equally distributed over the circumference. About 10 to 20 vertical measurement points N_z are required to measure the rapid decay of the *B*-field at upper and lower side of the pole plate. The vertical resolution may significantly be reduced in the middle part of the gap where the magnetic induction B is almost constant. Measurements at multiple radii are not required because the variations are less than 1 % as confirmed by additional experiments [10]. In total a useful scan of the *B*-field requires at least 100 measurement points.

RESULTS

The scanning process provides the radial component of the flux density

$$B(z_i, \varphi_k, r_0) \quad \begin{cases} i = 1 \ldots N_z \\ k = 1 \ldots N_\varphi \end{cases} \tag{3}$$

at points defined by vertical coordinate z_i and angle φ_i in cylindrical coordinates distributed in a particular grid depending on the thickness and position of the pole plate. Only in gaps with a circular geometry the radius r_0 is constant but in rectangular and otherwise shaped gap geometries the radius $r=f(z_i, \varphi_i)$ itself is a function of the other coordinates.

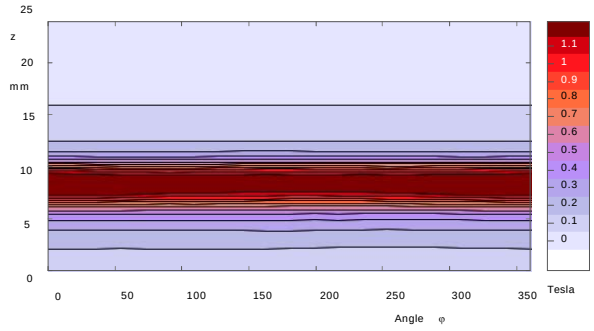

Figure 3: Contour plot of magnetic flux density versus vertical coordinate z and angle φ in the magnetic gap of loudspeaker A

For the calculation of the force factor $Bl(x)$ continuous values of the flux density

$$B(z,\varphi) = \frac{z_i - z}{z_i - z_{i-1}} B(z_{i-1}, \varphi_k, r_0) + \frac{z - z_{i-1}}{z_i - z_{i-1}} B(z_i, \varphi_k, r_0) \quad \begin{vmatrix} z_{i-1} < z < z_i \\ \varphi_{k-1} < \varphi < \varphi_k \end{vmatrix} \tag{4}$$

are derived from the discrete values by linear interpolation between the vertical coordinates z_i, while assuming constant values (steps) between the angles φ_i.

This interpolation allows to calculate the radial component $B(z, \varphi)$ at a cylindrical surface in the gap and to display the magnitude as a two-dimensional contour plot as shown for a magnetic system of loudspeaker A in Figure 3. There are significant variation versus z and only minor variation versus the angle φ which can be expected from an axial-symmetrical design.

To check the magnet system for asymmetries it is useful to depict the $B(z)$ versus the vertical coordinate z for selected angles φ_j as shown in Figure 4 or to display the $B(\varphi)$ versus angle φ for selected values of z_j as shown in Figure 5. The B value at an angle of φ =0° is a few percent higher than at φ =180°. Figure 5 also reveals that the asymmetry vanishes for positions above the pole plate (z > 9.7 mm) and persists below (z < 6.8 mm).

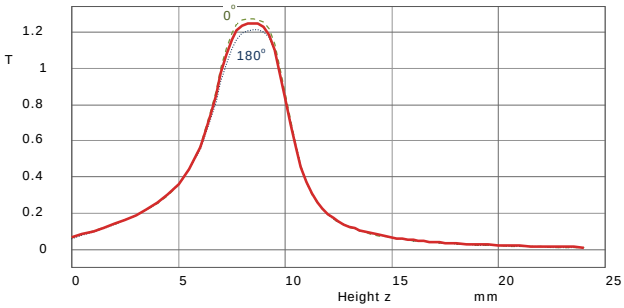

Figure 4: Magnetic flux density $B(z, \varphi_j)$ of loudspeaker A shown versus vertical coordinate z at two selected angles φ_j (dashed and dotted line) and compared with the mean value $\overline{B}^{\varphi}(z)$ (solid line).

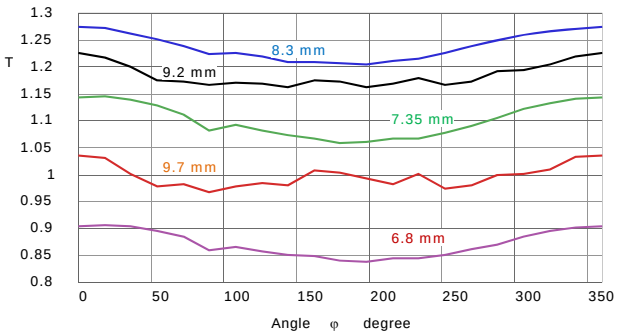

Figure 5: Magnetic flux density $B(z_i, \varphi)$ in the gap of loudspeaker A at selected heights z_i

DERIVED CHARACTERISTICS

The interpretation of the two-dimensional B distribution in the gap can be simplified by calculating further characteristics.

Mean Flux Density versus *z*

Assuming axial-symmetry of the magnetic circuit the motor design based on FEM provides a single value for

the flux density versus vertical coordinate z. A corresponding value derived from measurement is the mean flux density

$$\overline{B}^{\varphi}(z) = \frac{1}{2\pi}\int_0^{2\pi} B(z,\varphi)d\varphi$$
$$\overline{B}^{\varphi}(z_i) = \frac{1}{N_\varphi}\cdot\sum_{k=1}^{N_\varphi} B(z_i,\varphi_k) \qquad (5)$$

calculated by integrating $B(z,\varphi)$ over 2π or by calculating the mean value over all angles equally distributed on the circumference. Figure 4 also shows the mean value $\overline{B}^{\varphi}(z)$ as a solid line.

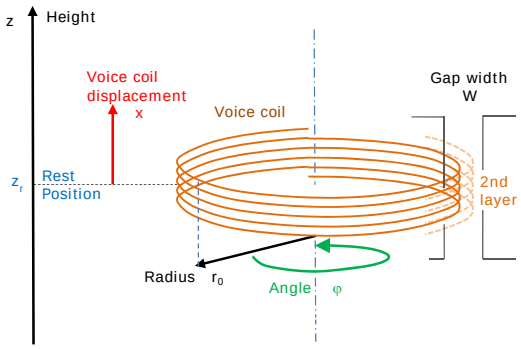

Figure 6: Calculation of the force factor by integrating the flux density B over the winding length l of the voice coil.

Force Factor

According to the basic Eq. (1) and Figure 6 the force factor which is a function of the voice coil displacement x from the rest position z_r

$$Bl(x) = m\int_{-N_w\pi}^{N_w\pi} B(x+\frac{\varphi}{2\pi}D+z_r,\varphi)\cdot r d\varphi$$
$$\approx m2\pi r\cdot\sum_{i=-N_w}^{N_w}\overline{B}^{\varphi}(x+\frac{iD}{2}+z_r) \qquad (6)$$

is calculated by integrating the flux density versus wire length l corresponding to an integration over both angle φ an windings N_w as illustrated in Figure 6. The parameter m represents the number of layers and D is the diameter of the wire including insulation and winding space.

Flux Density Variation

The asymmetry of the magnetic field in angular direction can be evaluated by the relative variation of the flux density

$$V_B(\varphi) = \frac{\overline{B}^{z}(\varphi) - \overline{\overline{B}^{\varphi}}^{z}}{\overline{\overline{B}^{\varphi}}^{z}}100\% \qquad (7)$$

using the mean value of the flux density

$$\overline{B}^{z}(\varphi) = \frac{1}{N_z}\sum_{k=1}^{N_z} B(z_k,\varphi) \qquad (8)$$

which is averaged over all vertical scanning points at a particular angle φ and the overall mean value

$$\overline{\overline{B}^{\varphi}}^{z} = \frac{1}{N_z}\sum_{k=1}^{N_z}\overline{B}^{\varphi}(z_k) \qquad (9)$$

which is averaged over all measurement points.

The variation of the flux density of loudspeaker A shown as solid line in Figure 7 reveals a maximal variation of 3 % which is a typical value of well-made transducers.

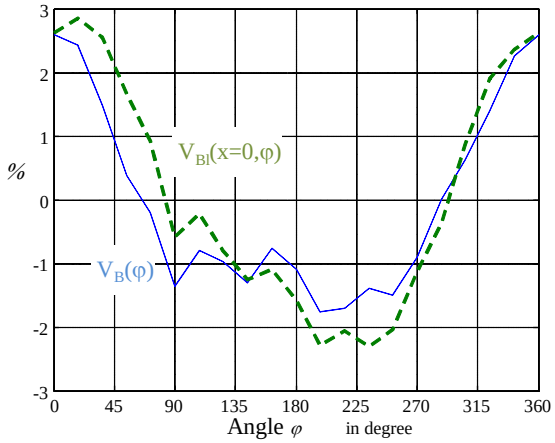

Figure 7: Relative variation of the flux density and force factor versus angle φ of loudspeaker A

Variation of Force Factor Distribution

Whereas the flux density variation $V_B(\varphi)$ considers variation accumulated over the total height z_H of scanned surface it is more practical to restrict the averaging range to the height of the voice coil and to calculate a new characteristic

$$V_{Bl}(x,\varphi) = \frac{2\pi Bl'(x,\varphi) - Bl(x)}{Bl(x)}100\% \qquad (10)$$

which describes the variation of the force factor distribution $Bl'(x,\varphi)$ versus angle φ on the circumference of the gap.

The force factor distribution

$$Bl'(x,\varphi) = mr\sum_{i=-N_w}^{N_w} B(x+\frac{iD}{2}+z_r,\varphi) \qquad (11)$$

is derived from equation (6) and the integral over the circumference gives the total force factor

$$Bl(x) = \int_0^{2\pi} Bl'(x,\varphi)\cdot d\varphi \cdot \qquad (12)$$

The variation $V_{Bl}(x,\varphi)$ of the force factor density of loudspeaker A is also depicted in Figure 7 and reveals that the driving force at angle φ=0° is about 5 % higher than at the opposite point at φ=180°.

DIRECT FORCE FACTOR MEASUREMENTS

The predicted force factor characteristic *Bl(x)* using the data of magnetic field scanning and coil geometry can be compared with the force factor directly measured in the assembled transducer by applying an audio-like stimulus and monitoring the electrical signals at the terminals. Nonlinear system identification [6] provides the dynamic force factor characteristic which represents both the static field generated by the magnet and the alternating field generated by the voice coil current.

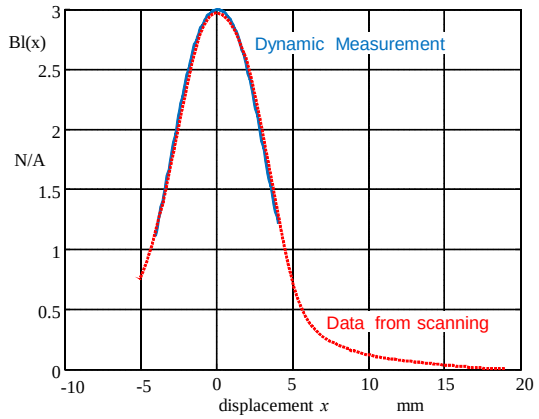

Figure 8: Force Factor *Bl(x)* versus voice coil displacement *x* of loudspeaker A calculated from scanned flux density and directly measured by dynamic method (large signal identification).

The static curve *Bl(x,i=0)* of loudspeaker A which neglects the effect of the voice coil current agrees well with the dynamic force factor characteristic *Bl(x, i>0)* as shown in Figure 8 because the small coil has a low inductance of 0.2 mH generating at maximal input current of 3 Ampere a relatively weak AC field which is only 5% of the static field generated by the magnet. However, transducers having a voice coil inductance larger than 1.5 mH and a peak current of more than 10 A produce an AC field which is in the same order of the magnitude as the DC field generated by the magnet. In this case the dynamic measurements provide an effective force factor curve which considers the constructive and destructive contribution of the AC field.

PRACTICAL DIAGNOSTICS

Although the dynamic *Bl(x)* measurement gives a more realistic shape of the force factor nonlinearity than the static methods the magnet field scanning provides some other valuable information for product development and loudspeaker diagnostics.

Verification of FEM

The mean flux density $\overline{B}^{\varphi}(z)$ calculated from many point collected by the scanning process as shown in Figure 4 is a convenient way to check the accuracy of the numerical magnet simulation using a static FEM model. This mean value is much more reliable than using a few points arbitrarily selected in the gap by manual measurements. Deviations between measured and predicted values of mean flux density may be caused by inaccurate material parameters and faults in the magnetization process.

Field Irregularities

Three-dimensional FEM can also cope with non-axial asymmetry and complicated shape of the iron and magnet system but usually lacks of information about geometrical deviations caused by metal forming, inaccurate assembling, material inhomogeneity and incomplete magnetization. Those failures can easily be detected by scanning the magnetic field as illustrated on loudspeaker B having a second neodymium disc glued slightly off centered on the pole piece.

The asymmetrical position causes a significant variation of the flux density versus angle φ as shown in the contour plot in Figure 9.

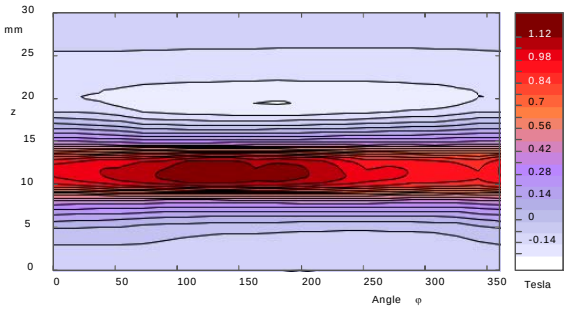

Figure 9: Contour plot of the magnetic flux density of loudspeaker B having a significant field asymmetry.

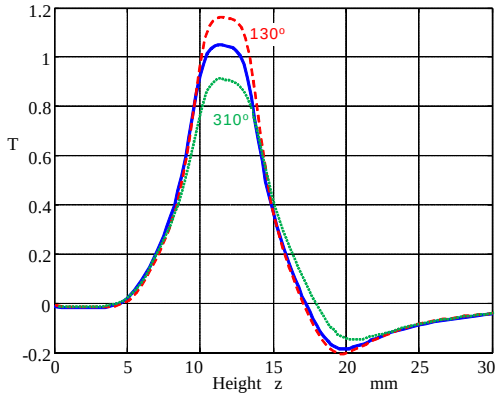

Figure 10: Mean value $\overline{B}^{\varphi}(z)$ (solid line) and values of the magnetic flux density at selected angles 130° (dashed line) and 310° (dotted line) versus vertical coordinate *z* of loudspeaker B.

Figure 10 reveals that the flux density inside the gap is increased at φ = 130° but reduced on the opposite side at 310°. In the fringe field above the gap at *z* = 20 mm the second magnet causes a negative value of the flux density

and an inverse dependency on angle φ. However, the windings for $z > 25$ mm are not affected by the negative fringe field.

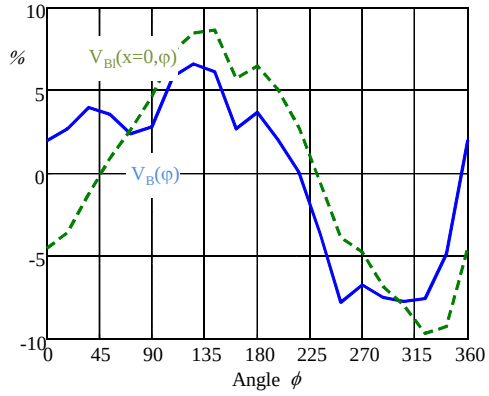

Figure 11: Relative variation of the flux density and force factor versus angle of loudspeaker B

The relative variation of the force factor in Figure 11 exceeds the variation of the flux density because the negative fringe field is not seen by the upper coil windings assuming a coil height of 7 mm and an excursion smaller than 5 mm. The angular variation of the force factor distribution corresponds to a difference of almost 18 % in the driving force on opposite sides of the coil. This unbalanced excitation may cause a rocking mode [11] of the cone as shown in Figure 12 which may cause voice coil rubbing in the gap generating impulsive distortion [12].

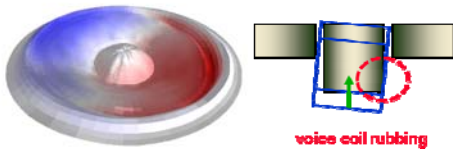

Figure 12: Rocking mode excited by an asymmetrical field

CONCLUSION

The flux intensity measured at the position of the voice coil gives valuable information about the magnet system of the transducer. The scanning process can be easily realized by using a Hall sensor and a three-axis positioning system changing the position of the sensor on a cylindrical grid providing sufficient resolution at the upper and lower side of the pole plate.

The mean flux density averaged over the circumference of the gap is a good criterion to verify the accuracy of numerical FEM and to check uncertainties of the material properties. Integrating the magnetic flux density on the voice wire gives the force factor characteristic $Bl(x,i=0)$ as a nonlinear function of voice coil displacement while neglecting the voice coil current i. The scanning of the magnetic DC field requires that the voice coil and other moving parts (cone, suspension) have been removed before injecting the Hall sensor into the gap. Due to the small clearance in the gap there is no space for measuring the magnetic AC field generated by the voice coil current directly. The results of nonlinear system identification showed that the AC field is negligible to the total flux density in micro-speakers, headphones, tweeters and other transducers having a small voice coil inductance. However, some subwoofers using larger coils require a dynamic FEM to explain the superposition of AC and DC field and current induced variation of the force factor characteristics at high voice coil current.

The scanning of the magnet field on the circumference of the gap seems to be the only way for detecting axial asymmetries and other irregularities of the magnetic field caused by material inhomogeneity and failures in manufacturing process such as partial magnetization and incorrect adjustment of the parts. The variation of force factor distribution in the gap reveals an asymmetrical driving force causing rocking modes and voice coil rubbing.

ACKNOWLEDGMENT

The author would like to thank Lars Neubert for experimental setup.

REFERENCES

[1] I. Aldoshina, et. al., “Loudspeaker Motor Nonlinear Modeling Based on Calculated Magnetic Field Inside the Gap,” presented at the 97th Convention of Audio Eng. Soc. 1994, preprint 3895.

[2] R. H. Small, “Assessment of Nonlinearity in Loudspeakers Motors,” in IREECON Int. Convention Digest (1979 Aug.), pp. 78-80.

[3] A. Dobrucki, “Non-typical Effects in an Electro-dynamic Loudspeaker with a Nonhomogeneous Magnetic Field in the Air Gap and Nonlinear Suspension,” J. Audio Eng. Soc., vol. 42, pp. 565 - 576, (July./Aug. 1994).

[4] M. Knudsen, et. al., “Determination of Loudspeaker Driver parameters Using a System Identification Technique,” J. Audio Eng. Soc. vol. 37, No. 9.

[5] D. Clark, "Precision Measurement of Loudspeaker Parameters,“ J. Audio Eng. Soc. vol. 45, pp. 129 – 140, (1997 March).

[6] W. Klippel, “Loudspeaker Nonlinearities - Causes, Parameters, Symptoms,“ J. Audio Eng. Society 54, No. 10 pp. 907-939 (2006 Oct.).

[7] G. Pellerin, et. al., “Finite Element Methods and Equivalent Electrical Models for Loudspeaker Characterization,” presented at the 114th Convention of Audio Eng. Soc. March 2003, preprint 5743.

[8] G. Loisos, A.J. Moses, “Critical evaluation and limitations of localized flux density measurements in

electrical steels," IEEE Transactions on Magnetics, July 2001, Volume: 37 Issue:4, pp. 2755 – 2757.

[9] W. Klippel, et.al., "Distributed Mechanical Parameters of Loudspeakers Part 1: Measurement," J. Audio Eng. Society 57, No. 9 pp. 696-708 (2009 Sept.).

[10] L. Neubert, "Statische Messung des magnetischen Feldes im Magnetfeld von Lautsprechern," Master Thesis, Hochschule für Technik und Wirtschaft, Dresden, 2010.

[11] W. Klippel, et.al., "Distributed Mechanical Parameters of Loudspeakers Part 2: Diagnostics," J. Audio Eng. Soc., vol. 57, No. 9 pp. 696-708 (2009 Sept.).

[12] W. Klippel, „Measurement of Impulsive Distortion, Rub and Buzz and other Disturbances", presented at the 114th Convention of the Audio Engineering Society, 2003 March 22–25, Amsterdam, The Netherlands, preprint # 5734.